JOURNAL OF APPLIED POLYMER SCIENCE VOL. 17, PP. 2191–2202 (1973)

Low-Angle X-Ray Scattering Investigation of Untreated and Alkali-Treated Jute

N. C. SAHU and D. MISHRA, *Department of Physics, Regional Engineering College, Rourkela, Orissa, India*

Synopsis

Pore analysis of untreated and alkali-treated samples of jute by the low-angle x-ray scattering method was made. The measurements were made using the low-angle scattering camera of the latest design by Kratky.[1] The theories of Kratky[2–4] and Porod[5–7] were used to evaluate and compare the various parameters of the scattering particles present in both types of jute fibers. Babinet's[8] reciprocal principle of scattering in optics was taken into account.

INTRODUCTION

Several workers[9–12] in the early thirties of this century observed that substances like protein fibers having polycrystals and colloidal powders show low-angle scattering. Guinier's[13] theory was extended for the study of colloidal particles of dilute systems where interference effects of the particles were neglected. Kratky,[1] however, pointed out during that time that the scattering by a dense assemblage of colloidal particles (micelles) is not independent of interparticle interference. A good amount of theoretical work has been put forward by Porod[6,7] and Kratky[2–4] in recent years, wherein they have emphasized pore analysis of the scattering particles in such systems, instead of determining particle dimensions.

We have used the low-angle scattering camera of latest design[1] capable of measuring size range of particles up to a Bragg value 20,000 Å and have been able to measure intensities up to a scattering angle as low as 10^{-3} radian, corresponding to a Bragg value of 12,000 Å. We have studied the nature of variation in the parameters of the scattering particles in the jute fibers when it was untreated (dewaxed) and when it was treated with 17.5% NaOH solution.[14,15,16] The results of the two samples were compared in an attempt to interpret the nature of variation in the fiber before and after alkali treatment.

EXPERIMENTAL

A Radon House x-ray apparatus with a Machlett A-2 x-ray diffraction tube of copper target was coupled with a highly sensitive voltage stabilizer. The x-ray unit was constantly operated at 30 KV and 20 mA throughout

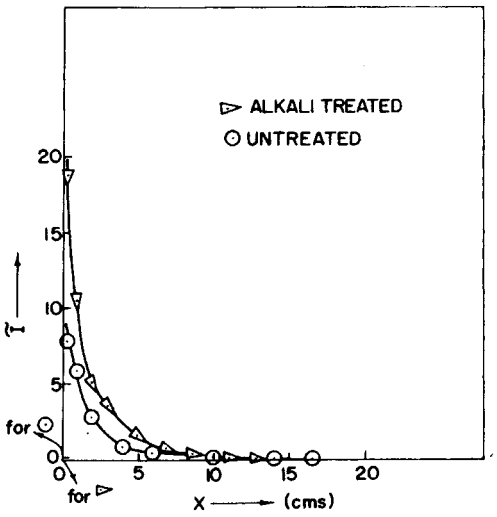

Fig. 1. Plot of $\tilde{I}$ vs. X: the scattering curves of the samples.

the experiment to obtain an intense x-ray beam. The beam was monochromatized by using a curved crystal monochromator after Johansson and Guinier[17,18] to obtain CuK_α radiation (λ = 1.54 Å). The entrance slit width of the camera used was 120 μ, providing high resolution. The photographic techniques as detailed in our previous papers[19,20] were adopted for recording of scattered intensities. A Moll microphotometer was used for measuring the intensities.

The Kratky camera uses a rectangular focus to get high intensities. Therefore, it would have necessitated a slit correction. But since the sample is a highly oriented one,[21] we can avoid such a correction by using smeared-out intensity $\tilde{I}$ for the evaluation of the parameters.[22] The values of $\tilde{I}$ and X are plotted for both samples in Figure 1. Here, X is a function of the scattering angle 2θ and is given by

$$X = 2ap\theta$$

where a is the sample film distance (here 230 mm) and p is the transformation ratio due to the microphotometer (here 100).

The jute sample was obtained through the Indian Jute Mills Association Research Institute, Calcutta. For dewaxing, defatting, and reducing the sample to a hohlraum system,[23] i.e., substances lying in layers with free spaces in between, we have adopted the same method as that of Roy.[24] This we call the untreated sample (dewaxed). For preparing the alkali-treated sample, short lengths of the dewaxed sample were soaked in 17.5% NaOH solution at a temperature of 25°C for 30 min. The dewaxed fibers, while still in the alkali bath, were stretched. The alkali was then drained off and the fibers were washed with water several times till they were neutral, and were then air dried.

THEORY AND DISCUSSION

The characteristic constants of the low-angle scattering curves of a sample with a good degree of orientation can reveal certain macromolecular parameters like specific inner surface, air fraction, and the transversal parameters. We evaluated here only such parameters that are common to both the dispersed and the dispersing phases, according to the methods of Porod[25] and Kratky,[26] as applied to a two-phase system where interparticle interference is predominant. The percentage of air present in the two samples will clearly give a picture of the textile properties of the untreated and alkali-treated fibers. Since we have used a transformation factor, $p = 100$, proper reduction has been made throughout while evaluating the parameters.

Air Fraction

The primary beam intensity (P_0) is given by

$$P_0 = \text{The area under the primary beam curve} \times \frac{\text{Exposure time of sample}}{\text{Exposure time of primary beam}}$$

The average value of P_0, obtained in the above manner by adopting the film shift device,[27] is equal to 463.8 cm^2, after taking the transformation factor into account.

The invariant Q, adopted by Debye and Bueche[28] and Porod[25] is defined by

$$Q = \int_0^\infty I(X)X^2dX \qquad \text{for slit-corrected intensity}$$

and

$$\tilde{Q} = \int_0^\infty \tilde{I}(X)XdX \qquad \text{for slit-smeared intensity.}$$

This is the case for a two-phase system, where Q is a characteristic function of the scattering curve and is independent of the shape and size of the scatterer but depends upon the scattering power, the mean square fluctuation of the electron density $\overline{\Delta\rho^2}$ of the two phases, and on the primary beam intensity P_0. Here,

$$\overline{\Delta\rho^2} = (\rho_1 - \rho_2)^2 w_1w_2$$
$$= \Delta\rho^2 w_1w_2$$
$$w_1 + w_2 = 1$$

where ρ_1, ρ_2 are the electron densities of the two phases, matter and void, respectively and w_1, w_2 are their volume fractions.

The invariant $\tilde{Q}$ of the scattering curve has been used by Kratky,[3] Porod,[25] and also by our group[19,20,29,30] for the determination of specific inner surfaces. In the present case, $\tilde{Q}$ was found by $\tilde{I}(X)X$ versus X curves and planimetering the area under the curve. The values thus obtained

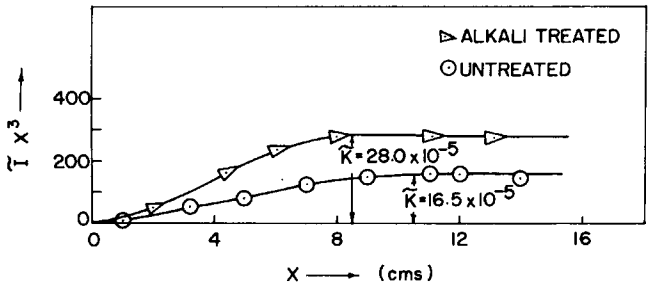

Fig. 2. Plot of $\tilde{I}\,x^3$ vs. X to find the characteristic constants $\tilde{K}$ of the samples.

are 40.4×10^{-4} cm^2 for the untreated sample and 83.8×10^{-4} cm^2 for the alkali-treated sample.

Kratky et al.[22] and Rothwell[31] have pointed out that the scattering curve with the smeared-out intensity $\tilde{I}$ has a decrease proportional to X^{-3} and X^{-4} for slit-corrected intensity, toward the very high angular range in the low-angle region. This is based on the fact that there is a homogeneous electron density distribution within each phase. Therefore, the curves $\tilde{I}(X)X^3$ versus X show an asymptotic behavior for large values of X. Thus,

$$\lim_{X\to\infty} \tilde{I}(X)X^3 = \tilde{K}$$

where $\tilde{K}$ is the characteristic constant, or the run constant of the curve. Thus, by exploiting the tail portion of the scattering curve, we get $\tilde{K}$ values (Fig. 2) for the two samples of 16.5×10^{-5} and 28.0×10^{-5}, respectively.

The correction of the scattering curve due to the fluctuation of the electron density as proposed by Luzzati, Witz, and Nicolaieff[32] has, however, not been taken into account because of the nonestablishment of a rigorous theory supporting their suggestions. We therefore proceed with the above expression as pointed out by Porod.[25]

The effective sample thickness D is given by Kratky[33]:

$$D = \frac{\delta_a}{\delta_c}\cdot\phi$$

where δ_c is the crystalline density of the jute fiber (whose constituents are mostly cellulosic). The value of δ_c is assumed to be 1.60 as suggested by Porod[34] for untreated sample and 1.59 for alkali-treated sample. Taking the apparent density δ_a as 1.48 and 1.5, respectively, for untreated and alkali-treated sample,[35] and ϕ, the inner diameter of the Mark capillary, as equal to 1.59 mm and 1.80 mm for the two samples, D values of 0.147 cm and 0.170 cm are obtained for the untreated and alkali-treated samples respectively.

Almost identical masses of the two samples were exposed to the x-ray beam. The electron density ρ is given by

$$\rho = \delta_c\frac{\sum O}{\sum A}$$

where $\sum O$ is the sum of the atomic number and $\sum A$ is the sum of the atomic weights. The values of ρ are calculated to be 0.85 and 0.84 in case of untreated and alkali-treated samples, taking $\sum O/\sum A$ as 0.53 for the untreated fibers by Kratky[36] and as 0.52 for the alkali-treated fibers as calculated by us.[20]

We assume that the sample contains air in order to account for the experimental values of the invariant

$$\tilde{Q}_{\text{exp}} = \int_0^\infty \tilde{I}(X) X dX$$

being equal to 40.4×10^{-4} cm^2 and 83.8×10^{-4} cm^2 in the two samples. The $\tilde{Q}_{\text{exp}}$ is compared with $\tilde{Q}_{\text{th}}$ obtained by the relation[37]

$$\tilde{Q}_{\text{th}} = \frac{7.9\times10^{-26}}{2\pi} \lambda^3 N^2 P_0 D \text{ (ap) } \rho^2 w_1 w_2$$

where N = Avogadro's number = 6.0228×10^{23} and the other symbols have their usual meanings.

For the calculation of air fraction, we have used the same procedure as used in an earlier paper[29] by our group. Now setting

$$\tilde{Q}_{\text{th}} = \tilde{Q}_{\text{exp}},$$

we obtain $w_1 w_2 = 0.214\times10^{-3}$ for the untreated sample and $w_1 w_2 = 0.392\times10^{-3}$ for the alkali-treated sample. Assuming $w_1 \simeq 1$ (approx.), we get a volume fraction of air w_2 of 0.214×10^{-3} and 0.392×10^{-3} in the two cases. Thus, the value of air fraction of the untreated sample is found to be 0.02% and that of the alkali-treated sample, 0.04%. The two different air fractions calculated in the two cases clearly show that the crystalline to noncrystalline ratio in the fiber is changed. This may throw light on some textile properties having close correlations between fiber crystallinity and certain physical properties such as density, tensile modulus, and ultimate tensile strength. This can also give some information about the fabric in assessing its value as clothing material.

Specific Inner Surface

The specific inner surface (O/V) defined as the phase boundary area per unit volume of the dispersed phase (per Å^3 of the sample volume) is calculated by using the Porod[25] relation

$$\frac{Q}{V} = \frac{8\pi}{\lambda a p} \cdot \frac{\tilde{K}}{\tilde{Q}_{\text{exp}}} \cdot w_1 w_2 = \frac{16.32}{ap} \cdot \frac{\tilde{K}}{\tilde{Q}_{\text{exp}}} \cdot w_1 w_2 \text{ for } \lambda = 1.54 \text{ Å}.$$

Now substituting the values of $\tilde{K}$ and $w_1 w_2$ for the samples, the specific inner surface of the untreated fiber is obtained as 6.2×10^{-6} Å^{-1} and that of the alkali-treated fiber, as 9.3×10^{-6} Å^{-1}. The values of the specific surface of the raw and 12.5% NaOH-treated fibers by the airflow method has been reported by Roy[35] to be 9.21×10^2cm^2/cm^3 and 11.52×10^2 cm^2/

cm^3, respectively. The order of this value agrees fairly well with the orders of our values.

Transversal Parameters

Besides amorphous cellulose, formation of open structures due to the combination of unremoved lignin with hemicellulose and air may be the cause of the void spaces in jute. The earlier reports of Statton[38] and Sen[39] reveal that the void volumes of jute are different from those of other celluloses. This may be due to the complicated structure of jute, as compared to that of pure cellulose. Since the scattering system like cellulose in jute is of complicated nature, one has to be content with finding some parameters giving a general characterization of size, polydispersity, and shape. In case of dry cellulose, Hermans et al.[40] have speculated that the shape of the scattering curves will largely be determined by the shape and size of the microvoids and will not provide information on the cellulosic substance itself. However, assuming a two-phase system of "matter" and "void," according to Babinet's[8] reciprocal relation, the scattering will be the same if "matter" and "void" exchange their positions. Thus, using the theories of Kratky[2-4] and Porod,[5-7] the complementarity of void and matter can also be employed to get a measure of the size of the scattering particles. In a system where the particles vary in shape and size, the x-ray scattering pattern can best yield certain size parameters and some broad features of the structure. The concept of size can be explained in the form of the average of the intersects, i.e., the chords cutting the two effective phases having uniform electron densities in each of them.[41] We then measure the average intersection lengths of these two phases as $\bar{l}_1$ and $\bar{l}_2$ for matter and void, respectively. These are also called transversal lengths and form a measure of the size of the phases.

In order to evaluate them from the scattering curve, we have to take note of the specific inner surface O/V. From geometric considerations, these transversal lengths are related to (O/V) as follows:

$$\bar{l}_1 = \frac{4\,w_1}{(O/V)}$$

and

$$\bar{l}_2 = \frac{4\,w_2}{(O/V)}.$$

The mean dimensions of the transversal lengths $\bar{l}_1$ and $\bar{l}_2$ are related to the range of inhomogeneity l_r as follows:

$$\frac{1}{l_r} = \frac{1}{\bar{l}_1} + \frac{1}{\bar{l}_2}$$

in analogy with the reduced mass in mechanics. Since $w_1 \simeq 1$ for the scattering material, $\bar{l}_r$ is equal to $\bar{l}_2$. Now, this l_r can be used for interpreting

certain results such as the size of the two phases building up the scattering system.

In the light of the above discussion, the values of $\bar{l}_2$ evaluated for the untreated and alkali-treated fibers are 137.7 Å and 168.7 Å, respectively. The values of $\bar{l}_1$ are 644.2 × 10^3 Å and 430.5 × 10^3 Å in the respective cases. The large variation in the values of these transversal lengths for the two fibers show the existence of anisotropy and polydispersity in the particles.

The concept of shape cannot be defined rigorously in case of a nonparticulate system. However, it is possible to speak of whether the scattering regions are isometric or anisometric in one or two dimensions. Thus, broadly we can distinguish three limiting cases of globular, fibrillar, and lamellar systems. The characteristic number f_c is defined as[25,29]

$$f_c = \frac{1}{2} \cdot \frac{l_c}{l_r}$$

where l_c is called the coherence length and l_r is the range of inhomogeneity. The increase in the ratio suggests a rising anisometry in the scattering system.

The length of coherence l_c derived from the scattering curve is given by the relation[25]

$$l_c = \frac{\lambda a p}{\pi} \frac{\int_0^\infty \tilde{I}(X)dX}{\int_0^\infty \tilde{I}(X)XdX} = \frac{\lambda a p}{\pi} \cdot \frac{\tilde{E}}{\tilde{Q}}$$

where $\tilde{E}$ is the integrated slit-smeared scattering energy and is given by

$$\tilde{E} = \int_0^\infty \tilde{I}(X)dX.$$

The values of $\tilde{E}$ for the untreated and the alkali-treated samples are obtained as 18.8 × 10^{-2} and 39.7 × 10^{-2} cm^2, respectively. On substituting the known values, we get l_c values in the above two cases as 524.5 Å and 533.9 Å.

From a knowledge of l_c and l_r, the characteristic number f_c in the untreated and alkali-treated fibers are obtained as 1.91 and 1.58. The decrease in the values of f_c shows that the anisometry is less in the alkali-treated fiber than in the untreated one, i.e., there is a more orderly arrangement of the micelles after alkali treatment.

Since the anisometry is not very large, the course of the scattering curve may be used in a reasonable low-angle region accessible for measurement, to determine the shape of the scattering system. Thus, the plot of $\tilde{I}(X)X^2$ versus X (Fig. 3), being a bell-shaped curve, shows that the scattering particles are lamellar in shape in accordance with the suggestions of Porod[41] and Hosemann and Bagchi.[42] We have drawn plots of $\tilde{I}(X)X^2$ versus X side by side for both fibers. Both show bell-shaped curves, the alkali-treated one having less pronounced flatness.

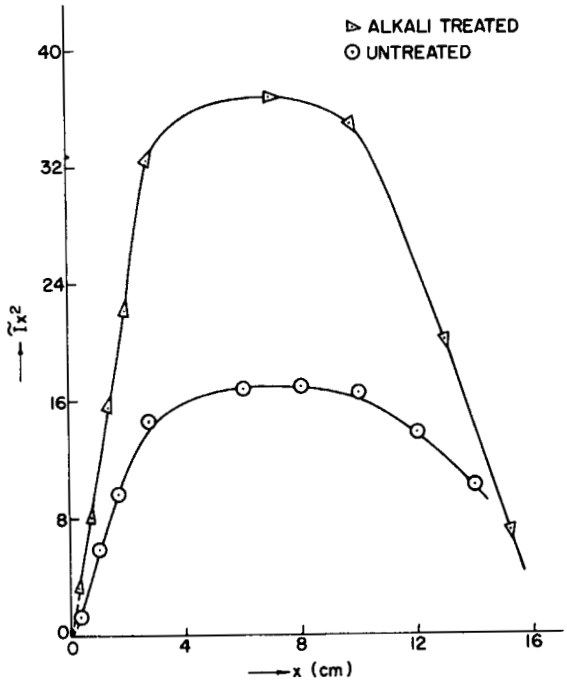

Fig. 3. Plot of $\tilde{I}\,x^2$ vs. X to study lamellar shape of the particles.

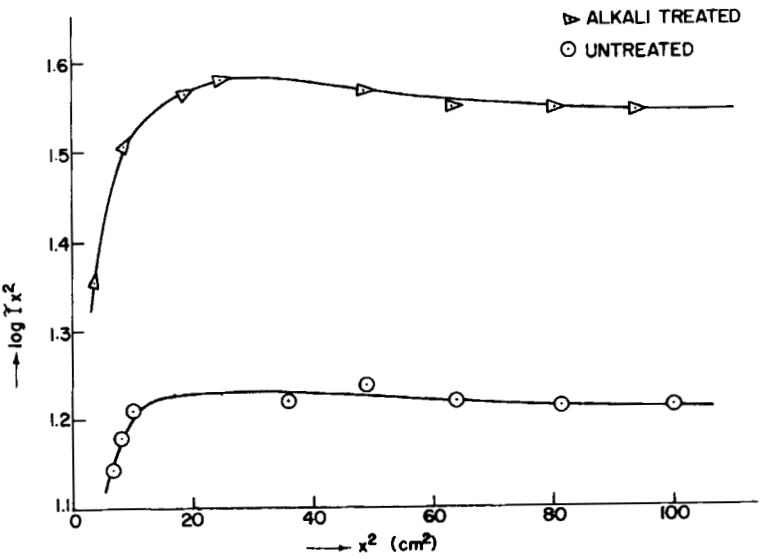

Fig. 4. Plot of log $\tilde{I}\,x^2$ vs. X^2.

TABLE I

Sample	$\tilde{Q}_{exp}$, $\times 10^{-4}$ cm²	$\tilde{E}$, $\times 10^{-2}$ cm²	$\tilde{K}$, $\times 10^{-5}$	Air, %	O/V, $\times 10^{-6}$ Å^{-1}	$\bar{l}_1$, $\times 10^3$ Å	$\bar{l}_2$, Å	l_c, Å	f_c
Untreated Jute (dewaxed)	40.4	18.8	16.5	0.02	6.2	644.2	137.7	524.5	1.908
Alkali-treated jute	83.8	39.7	28.0	0.04	9.3	430.5	168.7	533.9	1.580

The anisotropy and polydispersity in the particles play an important role. In a plot of log $\tilde{I}X^2$ versus X^2, its transition to a flat curve with decreasing scattering angle enables one to conclude that extended lamellae exist. The shape of such a curve deviates very little from a straight line unless there is strong polydispersity.[36] Though one cannot absolutely conclude that lamellar-shaped particles exist, yet the flatness of the curves log $\tilde{I}X^2$ versus X^2 (Fig. 4) at small angles indicates the presence of such lamellae in the fibers.

Such lamellar structures have been reported by Kratky et al.[36] in case of regenerated, air-swollen cellulose by small-angle x-ray scattering methods. Preston,[43] in his study of the size of the crystallites in natural cellulose, has observed such sheet-like structures mostly by using the method of x-ray wide-angle line-broadening and supported by low-angle scattering and electron microscopy method. Mukherjee and Woods[44] have also observed such sheet-like particles in cellulose fibers such as ramie, cotton, and jute by wide-angle x-ray and electron microscopy methods. These observations may stand as a supporting evidence for our findings of lamellar structures of the scattering particles in jute.

The evaluated results are presented in Table I.

CONCLUSIONS

Low-angle x-ray scattering has been applied in a very small-angular region to study jute fibers before and after treatment with 17.5% NaOH. Since cellulose, the main constituent of the fiber, is of complicated nature, and because of interparticle interference, emphasis has been placed, on pore analysis for finding certain parameters giving a general characterization of size, shape, and polydispersity. The main parameters studied are the specific inner surface, range of inhomogeneity, coherence length, the characteristic number, and the air fraction in the fiber before and after alkali treatment. The anisotropy and the polydispersity in the scattering particles have also been studied. Polydispersity is found to be low in the alkali-treated fiber compared to the dewaxed fiber. The steep nature of the scattering curve in the low-angle region shows the agglomeration of particles forming larger ones by rearrangement of micelles. Though there is a displacement of the maxima due to reorganization of micelles by alkali treatment, the shape of the scattering curve remains unchanged, behaving in a similar way as that for ramie and other fibers studied earlier by others.[45–47] The percentage of air fraction and the specific inner surface increase in the fiber after alkali treatment. This may be due to a decrease in the crystalline-to-noncrystalline ratio. The characteristic number decreases after treatment with 17.5% NaOH. The length of coherence remains almost the same, with a slight rise after treatment with alkali. The transversal parameters are changed after strong alkali-treatment. The fiber has lamellar-shaped particles in it, which becomes pronounced when the fiber is treated with alkali.

The authors express their sincere thanks to Prof. Dr. T. Ratho, Head of the Postgraduate Department of Physics, Regional Engineering College, Rourkela, Orissa, India, for his able guidance and helpful suggestions during the course of this work.

References

1. O. Kratky and Z. Skala, *Z. Elektrochem.*, **62**, 73 (1958).
2. O. Kratky, *Z. Naturforsch.*, **18**, 180 (1963).
3. O. Kratky, *Progr. Biophys.*, **13**, 106 (1963).
4. O. Kratky, private communication, 1971.
5. G. Porod, *Kolloid-Z.*, **133**, 16 (1953).
6. G. Porod, *Makromolec. Chem.*, **35**, 1 (1960).
7. G. Porod, *Proc. Conf. Small-Angle X-ray Scattering*, Syracuse, Gordon & Breach, New York, 1967, 1–15.
8. A. Guinier and G. Fournet, *Small-Angle Scattering of X-Rays*, Wiley, New York, 1955, p. 38.
9. P. Krishnamurthy, *Indian J. Phys.*, **5**, 473 (1930).
10. S. B. Hendricks, *Z. Kristallogr. Mineral*, **83**, 503 (1932).
11. H. Mark, *Physik und Chemie der Zellulose*, Springer, Berlin, 1932, p. 139.
12. B. E. Warren, *Phys. Rev.*, **49**, 885 (1936).
13. A. Guinier, *C. R. Hebd. Seances Acad. Sci.*, **204**, 1115 (1937).
14. M. M. Roy and M. K. Sen, *J. Text. Inst.*, **43**(8), T 396 (1952).
15. R. R. Mukherjee and H. J. Woods, *J. Text. Inst.*, **41**(11), T422 (1950).
16. S. C. Roy and S. Das, *J. Appl. Polym. Sci.*, **9**, 3427 (1965).
17. T. Johansson, *Z. Phys.*, **82**, 587 (1933).
18. A. Guinier, *C. R. Hebd. Seances Acad. Sci.*, **233**, 31 (1946).
19. T. Ratho and N. C. Sahu, *Kolloid-Z.*, **236**, 43 (1970).
20. T. Ratho and N. C. Sahu, *J. Colloid Interfac. Sci.*, **37**(1), 115 (1971).
21. V. D. Gupta, *J. Polym. Sci.*, **26**, 110 (1967).
22. O. Kratky, G. Porod, and Z. Skala, *Acta Phys. Austr.*, **13**(1), 76 (1960).
23. T. Ratho, N. C. Sahu, B. C. Panda, and T. Misra, *Ind. J. Pure Appl. Phys.*, **3**, 163 (1965).
24. S. C. Roy, *Text. Res. J.*, **30**, 451 (1960).
25. G. Porod, *Kolloid-Z.*, **124**, 83 (1951); *ibid.*, **125**, 51 (1952).
26. O. Kratky, *Kolloid-Z.*, **132**, 7 (1962).
27. O. Kratky, *Z. Anal. Chem.*, **201**, 161 (1964).
28. P. Debye and A. M. Bueche, *J. Appl. Phys.*, **20**, 518 (1949).
29. T. Ratho and B. C. Panda, *Ind. J. Phys.*, **39**, 207 (1965).
30. T. Ratho and T. Misra, *J. Polym. Sci. A-1*, **9**, 3491 (1971).
31. W. S. Rothwell, *J. Appl. Phys.*, **39**(3), 1840 (1968).
32. V. Luzzati, J. Witz, and A. Nicolaieff, *J. Mol. Biol.*, **3**, 367 (1961).
33. O. Kratky, *Trans. Faraday Soc.*, **52** (Part IV), 558 (1956).
34. G. Porod, private communication, May 1968.
35. M. M. Roy, *J. Text. Inst.*, **44**, T90 (1953).
36. O. Kratky and G. Miholic, *J. Polym. Sci.*, **2**, 449 (1963).
37. O. Kratky, G. Porod, A. Sekora, and B. Paletta, *J. Polym. Sci.*, **16**, 171 (1955).
38. W. O. Statton, *J. Polym. Sci.*, **22**, 385 (1956).
39. M. K. Sen, *Science and Culture*, **15**, 440 (1950).
40. P. H. Hermans, D. Heikens, and A. Weidinger, *J. Polym. Sci.*, **35**, 145 (1959).
41. P. Mittelbach and G. Porod, *Kolloid-Z.*, **202**, 40 (1965); G. Porod, *X-Ray Scattering from Irregular Structures*, Gordon & Breach, Science Publisher, New York, 1967, pp. 319–337.
42. R. Hosemann and S. N. Bagchi, *Direct Analysis of Diffraction by Matter*, N. H. Publishing Co., Amsterdam, 1962.

43. I. Nieduszynski and R. D. Preston, *Nature*, **225** (5229), 273 (1970).
44. S. M. Mukherjee and H. J. Woods, *Biochem. Biophys. Acta*, **10**, 499 (1953).
45. Janeschitz-Kreigel and O. Kratky, *Z. Elektrochem.*, **57**, 42 (1953).
46. T. Ratho and B. C. Panda, *Ind. J. Phys.*, **41** (12), 932 (1967).
47. O. Kratky, A. Sekora, and R. Treer, *Z. Elektrochem.*, **48**, 587 (1942).

Received August 22, 1972
Revised December 7, 1972